

duplicate

CORNELL AERONAUTICAL LABORATORY, INC.
BUFFALO, N. Y.

STABILITY OF SINGLE-TRACK VEHICLES

by

E. Döhring, Brunswick

Forschung Ing.-Wes. 21, no. 2, 50-62 (1955)

Translated
by

J. Lotsof

March 1957

STABILITY OF SINGLE-TRACK VEHICLES

by E. Döhring, Brunswick¹⁾

Forschung Ing.-Wes. 21, no. 2, 50-62 (1955)

Abstract. From a study of the equations of motion set up for a single-track vehicle it follows that three characteristic types of motion are possible for which the behavior of the vehicle can be theoretically stable or more or less unstable depending on the speed range. The method of calculation is applied to three different test machines. A separate consideration serves to explain the influence of the mechanical steering damper.

The development of the mechanism of single-track vehicles has been carried out with very little theoretical effort; the motorcycle mechanism reached its present form essentially through empirical designs. The possibilities of calculating this rather complicated configuration were surprisingly little known although F. Klein and A. Sommerfeld²⁾ had as early as 1890 undertaken the theoretical treatment of the bicycle with success. Indeed, with relatively little effort it is possible to measure the controllability of a motorcycle, which has already been manufactured, exclusively by tests in such a way that the usual characteristics follow because only two variables need to be considered, the rake angle and the castor trail. Without a doubt, however, knowledge of the theoretical relationships is very important for the designer if optimum performance is to be achieved and the mechanism is to be further perfected.

In the following the natural motion of a single-track vehicle, particularly the frequency of the natural oscillations about the condition of steady motion is calculated. The equations set up by F. Klein and A. Sommerfeld²⁾ for a bicycle we extended to be valid for a motorcycle as well.

1. Set-up of Linearized Equations of Motion

1.1 Notation

A single-track vehicle consists of two systems which can be rotated about a common axis (the steering axis): the front wheel with the fork, the handlebar, the light, the fender and the linkage; and the rear wheel with the frame, the motor and the rider who is considered rigidly attached to the frame. Let us not take into account the spring suspension of the wheels since only straight-line motion on a plane path in the neighborhood of upright equilibrium will be considered.

- 1) Report from the Institut für Fahrzeugtechnik of the Technische Hochschule at Brunswick.
- 2) F. Klein and A. Sommerfeld: the theory of the gyroscope. Vol. IV, Technical Applications. Berlin and Leipzig 1910.

Five coordinates are necessary to determine the position of the vehicle: two coordinates establish the point of contact of the rear wheel, two angles give the attitude of the plane of the wheel, and one coordinate determines the angle between the frame and the plane of the forward wheel. There is an additional requirement that both wheels must touch the ground. With five degrees of positional freedom, the vehicle nevertheless has only three motion degrees of freedom: leaning of the plane of the frame (roll), rotation of the hinged parts about the steering axis, and the forward motion whose direction has already been determined by the position of the front wheel. Thus, as in all systems with rolling motion, we are dealing with a non-holonomic system, i.e. the vehicle can arrive at any of its ∞^5 positions through a series of permissible motions, but it cannot reach every infinitely close position by an infinitely small motion.

The calculation is carried out for small angles since integration of the equations of motion, after substitution of the non-holonomic rolling condition, is possible only after they are linearized. The notations, part of which are shown in Fig. 1 and 2, are:

a	Distance of the imaginary separation point between the front and rear wheel system from the point of contact of the front wheel
c_1, c_2	Distance between the point where the steering axis intersects the ground and the point of contact of the front wheel (castor trail) and the rear wheel, respectively
C_1 to C_3	Constants
$Fr = v/\sqrt{g l}$	Froude number
g	Gravitational acceleration
h	Height of point of application of reaction force Y
h_1, h_2	Distance of the front and rear wheel system center of gravity, respectively, from the track
J_1, J_2	Mass moment of inertia of the front and rear wheel system, respectively
k	Radius of gyration
$K = k/l$	Inertia ratio
$l = c_2 - c_1$	Wheel base
L	Wave length
m_1, m_2	Mass of front and rear wheel systems, respectively
m_{1R}, m_{2R}	Reduced mass of front and rear wheel with motor
$M = m_1/m_2$	Mass ratio
M_D, M_R	Reaction moment of the steering damper and of the forward wheel system, respectively
N_1, N_2	Angular momentum of front and rear wheel, respectively
r	Horizontal distance between the point of application of Y and the vertical through the front wheel point of contact
r_1, r_2	Distance from the projection of the c.g. onto the track to the point of contact of the front and rear wheel, respectively
R	Effective radius of front and rear wheel
s_1, s_2	Distance from the front and rear wheel c.g. to the parallel to the steering axis passing through the corresponding point of contact
t	Time
U, V, W	Space-fixed coordinates
v	Velocity
x, y, z	Body-fixed coordinates
Y	Reaction force acting on the steering axis in the vertical direction (y direction)
Y_1, Y_2	Vertical reaction force acting at the point of contact of the front and rear wheel, respectively

z	Reaction force acting in the steering axis normal to the plane of the wheel
α, β	Real and imaginary part of Ω
γ	Handlebar deflection angle
θ_1, θ_2	Tilt angle of the front and rear wheel, respectively, with respect to vertical (bank angle)
λ	Frequency parameter
σ	Rake angle
τ	Reduced time
φ_1, φ_2	Angle between the front and rear wheel, respectively, and the mean plane in the direction of motion
$\psi = \varphi_1 - \varphi_2$	Angle between planes of front and rear wheels (steering angle)
ω	Angular velocity of a wheel
Ω	Reduced frequency with roots Ω_1 to Ω_4 .

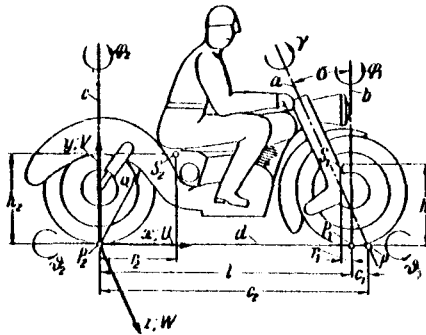


Fig. 1 Single-Track Vehicle

a Steering axis, b Vertical through the point of contact P_1 of the front wheel, c Vertical through the point of contact P_2 of the rear wheel, d Track, P Point of intersection of a with the road, S_1 and S_2 Center of gravity of front and rear wheel system, resp. σ Rake Angle (angle between a and b), γ Steering deflection angle about a, φ_1 and φ_2 Angle between front and rear wheel planes, resp., and the mean plane of motion, θ_1 and θ_2 Tilt angle of front and rear wheel planes with respect to vertical, h_1 and h_2 distance from points S_1 and S_2 to d, r_1 and r_2 Distance from the projection of c.g. on d to point of contact of front and rear wheel, $c_1 = \overline{P_1P}$ Castor trail, $c_2 = \overline{P_2P}$, $l = \overline{P_1P_2} = c_2 - c_1$ Wheelbase; x, y, z Body-fixed coordinate system; U, V, W Spaced-fixed coordinate system, \bar{o} rotation vector

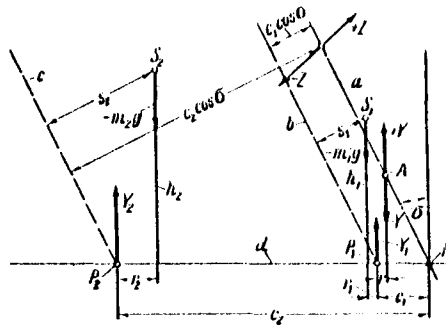


Fig. 2 Forces on Single-Track Vehicle

$a, d, P_1, P_2, P, S_1, S_2, \sigma, h_1, h_2, r_1, r_2, c_1, c_2$ as in Fig. 1. Also: b and c Parallels to a through P_1 and P_2 , A Point of application of the vertical reaction force Y , r Horizontal distance between A and P_1 , s_1 Distance of point S_1 from b , s_2 Distance of point S_2 from c , m_1 and m_2 Mass of front and rear wheel systems, resp. g Gravitational acceleration, Y Vertical reaction force in the steering axis, Z Reaction force acting on the steering axis normal to wheel plane, Y_1 and Y_2 Vertical reaction force at P_1 and P_2

1.2 Geometric Relations

There is a geometric relationship between the tilt angles θ_1 and θ_2 of the front and rear wheels, respectively. If we consider the motorcycle with undeflected handlebar to be rolled to the right³⁾, for example $\theta_1 = \theta_2$. Let the angle γ be the handlebar deflection angle, measured about the steering axis (considered as axis of rotation of the hinged parts); let it be positive to the left and negative to the right. Now if the handlebar is turned to the right (through $-\gamma$), then the tilt of the front wheel increases because of the inclination of the steering axis through the rake angle σ with respect to vertical; the increase is the component of the angle γ about the track. According to the laws of small rotations, this component has the value $-\gamma \sin \sigma$. Hence

$$\theta_1 - \theta_2 = \gamma \sin \sigma \dots \dots \dots (1).$$

The component of the angle γ about the vertical axis amounts to $\gamma \cos \sigma$ and is equal to the angle $\phi_1 - \phi_2$ between the planes of the front and rear wheels with respect to the plane of the mean direction of motion (cf. Fig. 1):

$$\phi_1 - \phi_2 = \gamma \cos \sigma \dots \dots \dots (2).$$

1.3 Determination of the Non-holonomic Relationship

Consideration of the features of the motion leads to the non-holonomic rolling conditions which is still required, Fig. 3. If the velocity v of the front wheel in its track and its angular velocity $\dot{\phi}_1 = d\phi_1/dt$ about the vertical are regarded as given, then the motion of the rear wheel is also determined. For the rear wheel is hinged at the point of intersection P of the steering axis (with the road) which moves with the front wheel and must always follow this point. The point of intersection P has a velocity

3) Terms like right or left are always with respect to a driver sitting in the seat.

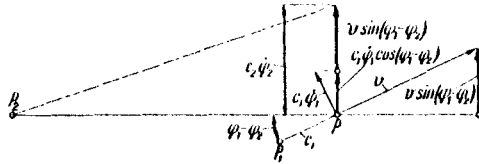


Fig. 3 Velocities for Single-Track Vehicle

P, P₁, P₂, c₁, c₂, φ₁, φ₂, as in Fig. 1; also: v Velocity of the front wheel, φ̇₁ = dφ₁/dt, φ̇₂ = dφ₂/dt

v in the track of the front wheel and a velocity c₁ φ̇₁, normal to the plane of the front wheel since it rotates at a rate φ̇₁ about the point of contact P₁ (between the wheel and the road) which is a distance c₁ = P₁P from P. The distance c₁, the so-called castor trail, is one of the most important quantities of the system. The track of the rear wheel makes an angle φ₁ - φ₂ with that of the front wheel. The point P therefore has a component of motion of

$$c_1 \dot{\varphi}_1 \cos(\varphi_1 - \varphi_2) + v \sin(\varphi_1 - \varphi_2) \dots (3)$$

normal to the track of the rear wheel. This component of motion of the point of intersection can also be expressed in terms of its distance c₂ from the point of contact P₂ of the rear wheel and the angular velocity φ̇₂ = dφ₂/dt of the plane of the frame about a vertical axis. Thus for small angles we have the non-holonomic condition

$$c_2 \dot{\varphi}_2 = c_1 \dot{\varphi}_1 + v(\varphi_1 - \varphi_2) \dots (4)$$

The velocity component v* of point P in the direction of the rear wheel track

$$v^* = v \cos(\varphi_1 - \varphi_2) - c_1 \dot{\varphi}_1 \sin(\varphi_1 - \varphi_2) \dots (5),$$

differs from v only in second order quantities.

1.4 Determination of the Applied Forces

The forces which act on the vehicle and the reaction forces will now be determined. Forces acting up are positive; those acting down are negative. With g as gravitational acceleration and with m₁ and m₂ as masses of the front and rear wheel systems, respectively, the two mass forces m₁g and m₂g act at the centers of gravity S₁ and S₂. Reaction forces act at the two points of contact and at the steering joint (bearing of fork in the frame).

For the vertical reaction forces it is only necessary to consider the forces which oppose the weight during rectilinear motion under equilibrium conditions since, for small deviations from rectilinear motion, they suffer only small changes of higher order. The vertical force

$$Y_2 = m_2 g \{(l - r_2)/l\} + m_1 g (r_1/l) \dots (6),$$

acts at the point of contact of the rear wheel and the vertical force

$$Y_1 = m_2 g (r_2/l) + m_1 g \{(l - r_1)/l\} \dots (7).$$

acts at the point of contact of the front wheel. Here r_1 and r_2 are the horizontal distances of the centers of gravity from the points of contact and l is the so-called wheelbase, cf. Fig. 1 and 2. At the steering joint a reaction force and a reaction moment must be applied. A vertical force

$$-Y = Y_2 - m_2 g = -m_2 g (r_2/l) + m_1 g (r_1/l) \dots (8).$$

acts on the front wheel system.

$$Y = -Y_2 + m_2 g = m_2 g (r_2/l) - m_1 g (r_1/l) \dots (9).$$

acts on the frame. If the imaginary point of separation between the front and rear wheel systems is a distance a behind the front point of contact P_1 , then the reaction moment acting on the front wheel system (right hand rotation positive) is

$$M_R = Y_2(l - a) - m_2 g (l - a - r_2) \dots (10).$$

The corresponding reaction moment acting on the frame is $-M_R$.

However, the thrust bearing can be built in at any arbitrary point on the steering axis and hence by a displacement on the steering axis the vertical force and moment can be expressed as a single force. For $M_R = 0$ it follows from Eq. (10) and (8) that

$$a = m_1 r_1 l / (-m_2 r_2 + m_1 r_1) \dots (11).$$

The vertical reaction forces are then to be applied at the steering axis at a distance

$$r = -a - m_1 r_1 l / (m_2 r_2 - m_1 r_1) \dots (12)$$

ahead of the forward point of contact. The height of the point of application of these reaction forces is

$$h = (c_1 - r) \operatorname{ctg} \sigma = \left(c_1 - \frac{m_1 r_1 l}{m_2 r_2 - m_1 r_1} \right) \operatorname{ctg} \sigma \quad (13).$$

The horizontal reaction forces will now be determined. The forces $+Z$ which transmit the lateral motion, act at the steering axis normal to the plane of the wheel. Their magnitude depends on the instantaneous state of the motion and can only be determined if the form of the motion is known. In any case, they are of first order and must therefore be considered. The height of their point of application is not needed.

In addition, there are reaction forces acting on the steering axis in the direction of motion; they transmit the forces which are necessary to drive the front wheel. If the resistance of the front wheel to rolling and forward motion is neglected, then for rectilinear motion under equilibrium conditions these reaction forces vanish, and for small deviations from these conditions, they are of second order.

For a handlebar deflection away from the middle position, the center of gravity S_1 and S_2 move down slightly. However, this gives rise only to terms of second order which will not be considered here. The corresponding force terms nevertheless enter the equations of motion through the reaction forces Y at the steering axis (cf. below, Section 1.6). Centrifugal forces $m_1 v \dot{\phi}_1$ and $m_2 v \dot{\phi}_2$ act at the centers of gravity S_1 and S_2 and perpendicular to the planes of the wheels.

The angular momentum N of the wheels depends on their mass moment of inertia J , their angular velocity ω , and their effective radius R

$$N = J \omega = J v / R \dots \dots \dots (14).$$

The angular momentum of the motor is to be added to that of the rear wheel if the engine rotates in the same direction as the wheel; if the direction of rotation is opposite, then the momentum of the wheel is decreased by that of the motor. It is useful to regard the angular momentum of the motor as an increase or decrease of the moment of inertia of the rear wheel (taking into account the gearing ratio between the wheel and the motor). Thus for the front wheel we have $N_1 = J_1 v / R$ and for the rear wheel with the motor $N_2 = J_2 v / R$. The effective radii are equal for the front and rear wheels.

A rolling motion about the track sets up a gyroscopic force about a vertical axis; at the rear wheel with $\dot{\theta}_2 = d \theta_2 / dt$ its magnitude is $- N_2 \dot{\theta}_2$ and at the front wheel with $\dot{\theta}_1 = d \theta_1 / dt$ its magnitude is $- N_1 \dot{\theta}_1$. Rotation about a vertical axis sets up a gyroscopic moment about the track; it is $N_2 \dot{\phi}_2$ for the rear wheel and $N_1 \dot{\phi}_1$ for the front wheel.

In order to be able to write down the equation of motion, we must determine the time rate of change $\dot{\mathcal{B}}_p$ of the angular momentum vector \mathcal{B}_p about the axis of rotation; this must be equal to the moment \mathcal{M}_p about this axis. The space-fixed coordinate system is designated by U, V, W and the body-fixed system by x, y, z (cf. Fig. 1). With $\bar{\omega}$ as angular velocity vector of the front and rear wheel system about the points of contact and \mathcal{B}_{rel} as angular momentum vector with respect to the body-fixed coordinate system, we have

$$\dot{\mathcal{B}}_p = \dot{\mathcal{B}}_{rel} + \bar{\omega} \times \mathcal{B} = \mathcal{M}_p \dots \dots \dots (15).$$

The angular velocity vector $\vec{\omega}$ has component $\dot{\theta}$, $\dot{\phi}$, and 0 in the x, y, and z directions. Here θ and ϕ are written instead of θ_1 and θ_2 or ϕ_1 and ϕ_2 . With J_{xx} and J_{yy} as mass moments of inertia of the system about the x and y axes, and with J_{xy} , J_{xz} and J_{yz} as products of inertia in the xy, xz and yz planes respectively, the angular momentum \mathcal{B} is composed of the corresponding components $J_{xx} \dot{\theta} - J_{xy} \dot{\phi}$, $- J_{xy} \dot{\theta} + J_{yy} \dot{\phi}$ and $- J_{xz} \dot{\theta} - J_{yz} \dot{\phi}$, respectively.

The cross product $\vec{\omega} \times \mathcal{B}$ leads to terms in which the angular velocity occurs as a second order term. Road tests show that for the natural motions under consideration the angular velocity can also be regarded as small and hence quadratic velocity terms may be neglected. Thus, for the components \dot{B}_U , \dot{B}_V , \dot{B}_W of the time rate of change of angular momentum \mathcal{B}_P in the U, V, and W directions with M_U , M_V , and M_W as corresponding components of \mathcal{M} and with $\ddot{\theta} = d^2 \theta / dt^2$, and $\ddot{\phi} = d^2 \phi / dt^2$, we get

$$\left. \begin{aligned} J_{xx} \ddot{\theta} - J_{xy} \ddot{\phi} &= M_U = \dot{B}_U, \\ - J_{xy} \ddot{\theta} + J_{yy} \ddot{\phi} &= M_V = \dot{B}_V, \\ - J_{xz} \ddot{\theta} - J_{yz} \ddot{\phi} &= M_W = \dot{B}_W \end{aligned} \right\} \dots (16).$$

The component M_W in the W direction causes a change in the reaction force $+Y$, but this will be regarded as small and of first order with respect to the gravity force, so that its moment about the axis to be considered remains second order.

The equations of motion can now be stated for the two systems for the U axis (the track). In doing this, we should immediately add the two equations algebraically since vectorial addition will result in terms of second order only because it has been assumed that the angle $\phi_1 - \phi_2$ between the tracks of the two wheels is small.

1.5 Equation of Motion for Rolling about the Track

For small angles and with J_{1U} and J_{2U} as moments of inertia of the front and rear wheel system about the track, J_{1UV} and J_{2UV} as products of inertia of the front and rear wheel systems in the plane of the wheels, N_1 and N_2 as angular momentum of the front and rear wheels, and with m_1 and m_2 as mass of the front and rear wheel systems, respectively, the equation of motion for rolling of the vehicle about its track is

$$\left. \begin{aligned} J_{1U} \ddot{\theta}_1 + J_{2U} \ddot{\theta}_2 - J_{1UV} \ddot{\phi}_1 - J_{2UV} \ddot{\phi}_2 &= N_1 \dot{\phi}_1 + \\ + N_2 \dot{\phi}_2 + v(m_1 h_1 \dot{\phi}_1 + m_2 h_2 \dot{\phi}_2) + m_1 g h_1 \theta_1 + \\ + m_2 g h_2 \theta_2 + Y(c_1 - r) \theta_1 \operatorname{ctg} \sigma - Y(c_1 - r) \theta_2 \operatorname{ctg} \sigma \end{aligned} \right\} (17)$$

or with Y given by Eq. (9)

$$\left. \begin{aligned} J_{1U} \ddot{\theta}_1 + J_{2U} \ddot{\theta}_2 - J_{1UV} \ddot{\phi}_1 - J_{2UV} \ddot{\phi}_2 &= N_1 \dot{\phi}_1 + \\ + N_2 \dot{\phi}_2 + v(m_1 h_1 \dot{\phi}_1 + m_2 h_2 \dot{\phi}_2) + \\ + g(m_1 h_1 \theta_1 + m_2 h_2 \theta_2) + \\ + g \left(m_2 \frac{r_2}{l} - m_1 \frac{r_1}{l} \right) (c_1 - r) (\theta_1 - \theta_2) \operatorname{ctg} \sigma \end{aligned} \right\} (18).$$

If the kinematic condition of Eq. (1) is introduced, then the last term of Eq. (18) can be written

$$-y \left(m_2 \frac{r_2}{l} - m_1 \frac{r_1}{l} \right) (c_1 - r) \gamma \cos \sigma$$

it vanishes if the front and rear wheels lie in a plane, and corresponds to the drop in c.g. with handlebar deflection, which has already been mentioned.

1.6 Moments about Axes Parallel to the Steering Axis

It would now appear appropriate to set up the equation of motion for rotation about vertical axes. However, it is better not to use these axes, but rather those which are parallel to the steering axis and pass through the points of contact (cf. b and c in Fig. 2). We also set up the equations for the two systems separately in order to achieve better insight. In doing this, the reaction forces at the point of separation must be taken into account. At that point the forces $+Z$ act normal to the plane of the wheel and $+Y$ act in a vertical direction. In addition, the reaction moment of a steering damper must be introduced into the calculation. In this connection we are dealing with a rotational moment about axes parallel to the steering axis; it is $-M_D$ on the hinged part and $+M_D$ on the frame. The moment is introduced through a friction damper and is therefore to be considered constant. The variations which arise in practice because of the difference between coulomb and sliding friction will not be considered.

The reaction forces $+Y$ and $+Z$ set up a moment $(Z + Y \theta_2) c_2 \cos \sigma$ about a line through P_2 and parallel to the steering axis, and $-(Z + Y \theta_1) c_1 \cos \sigma$ about a parallel line through P_1 . A small rotation about the steering axis or an axis parallel to it can be broken down into a component about a vertical line (which enters into the calculation as a cosine component) and a component about the track (as sine component which is negative because the roll resulting from a handlebar deflection will be to the left, in the direction of negative rotation of the roll angle θ). The corresponding components of the mass forces about the vertical and about the track oppose these component rotations. For the front wheel system, the tire rate of change \dot{B}_{St} of the angular momentum B_{St} about the steering axis with J_{1V} as moment of inertia of the front wheel system about a vertical axis through P_1 is given by the relation

$$\begin{aligned} \dot{B}_{St} &= \dot{B}_V \cos \sigma - \dot{B}_U \sin \sigma = \\ &= (J_{1V} \ddot{\varphi}_1 - J_{1UV} \ddot{\theta}_1) \cos \sigma - \\ &\quad - (J_{1U} \ddot{\theta}_1 - J_{1UV} \ddot{\varphi}_1) \sin \sigma \end{aligned} \quad \left. \dots \dots (19) \right\}$$

One component of the gyroscopic moment about the steering axis or parallels to it arises from the rolling of the machine at a rate $\dot{\theta}$ about the track (cosine component), and the second comes from a rotation about a vertical at a rate $\dot{\varphi}$ (sine component); both act in a negative direction about the steering axis and give

$$-N_1 (\dot{\theta}_1 \cos \sigma + \dot{\varphi}_1 \sin \sigma).$$

In addition the moments due to centrifugal force, gravity and the reaction forces Z and Y must be considered. The lever arm of the centrifugal force is (cf. Fig. 2)

$$s_2 = h_2 \sin \sigma + (r_2 / \cos \sigma) \dots \dots \dots (20)$$

for the frame system, and

$$s_1 = h_1 \sin \sigma - (r_1 / \cos \sigma) \dots \dots \dots (21).$$

for the front wheel system.

1.7 Equation of Motion for Rotation about the Steering Axis

The equation of motion for rotation of the front wheel system about the steering axis is then

$$\left. \begin{aligned} (J_{1V} \ddot{\varphi}_1 - J_{1UV} \ddot{\vartheta}_1) \cos \sigma - (J_{1U} \ddot{\vartheta}_1 - J_{1UV} \ddot{\varphi}_1) \sin \sigma = \\ = -N_1 (\dot{\vartheta}_1 \cos \sigma + \dot{\varphi}_1 \sin \sigma) - m_1 s_1 v \dot{\varphi}_1 - \\ - m_1 g s_1 \vartheta_1 - Y c_1 \vartheta_1 \cos \sigma - Z c_1 \cos \sigma - M_D \end{aligned} \right\} \dots (22)$$

and the corresponding equation for the rear wheel system with J_{2V} as moment of inertia of the rear wheel system about the vertical axis through P_2 is

$$\left. \begin{aligned} (J_{2V} \ddot{\varphi}_2 - J_{2UV} \ddot{\vartheta}_2) \cos \sigma - (J_{2U} \ddot{\vartheta}_2 - J_{2UV} \ddot{\varphi}_2) \sin \sigma = \\ = -N_2 (\dot{\vartheta}_2 \cos \sigma + \dot{\varphi}_2 \sin \sigma) - m_2 s_2 v \dot{\varphi}_2 - \\ - m_2 g s_2 \vartheta_2 + Y c_2 \vartheta_2 \cos \sigma + Z c_2 \cos \sigma + M_D \end{aligned} \right\} \dots \dots \dots (23).$$

From Eq. (22) and (23), by eliminating the unknown reaction force Z, we get the equation of motion for rotation about the steering axis

$$\left. \begin{aligned} c_2 [(J_{1V} \cos \sigma + J_{1UV} \sin \sigma) \ddot{\varphi}_1 - (J_{1UV} \cos \sigma + \\ + J_{1U} \sin \sigma) \ddot{\vartheta}_1] + c_1 [(J_{2V} \cos \sigma + J_{2UV} \sin \sigma) \ddot{\varphi}_2 - \\ - (J_{2UV} \cos \sigma + J_{2U} \sin \sigma) \ddot{\vartheta}_2] = -[(N_1 \dot{\vartheta}_1 c_2 + \\ + N_2 \dot{\vartheta}_2 c_1) \cos \sigma + (N_1 \dot{\varphi}_1 c_2 + N_2 \dot{\varphi}_2 c_1) \sin \sigma] - \\ - v (c_2 m_1 s_1 \dot{\varphi}_1 + c_1 m_2 s_2 \dot{\varphi}_2) - g (c_2 m_1 s_1 \vartheta_1 + \\ + c_1 m_2 s_2 \vartheta_2) + \\ + g c_1 c_2 (\vartheta_2 - \vartheta_1) \left(m_2 \frac{r_2}{l} - m_1 \frac{r_1}{l} \right) \cos \sigma + (c_1 - c_2) M_D \end{aligned} \right\} (24)$$

1.8 Introduction of the Non-holonomic Equation

With $c_2 - c_1 = \mathcal{L}$ and setting $\varphi_1 - \varphi_2 = \psi$, $\dot{\varphi}_1 - \dot{\varphi}_2 = \dot{\psi}$ and $\ddot{\varphi}_1 - \ddot{\varphi}_2 = \ddot{\psi}$ we get the following forms from Eq. (4):

$$l \dot{\varphi}_1 = v \psi + c_2 \dot{\psi} \dots \dots \dots (25),$$

$$l \dot{\varphi}_2 = v \psi + c_1 \dot{\psi} \dots \dots \dots (26),$$

$$l \ddot{\varphi}_1 = v \ddot{\psi} + c_2 \ddot{\psi} \dots \dots \dots (27)$$

and

$$l \ddot{\varphi}_2 = v \ddot{\psi} + c_1 \ddot{\psi} \dots \dots \dots (28).$$

By means of Eq. (25) to (28) the angles φ_1 and φ_2 together with their derivatives can be expressed in terms of ψ in the equations of motion. If we also note the fact that $\psi = \gamma \cos \sigma$ and hence, from Eq. (1),

$$\vartheta_1 - \vartheta_2 = -\psi \operatorname{tg} \sigma \dots \dots \dots (29)$$

then instead of Eq. (18) we get the following equation for rolling about the track

$$\left. \begin{aligned} & J_{1U} \ddot{\vartheta}_1 + J_{2U} \ddot{\vartheta}_2 - \frac{J_{1UV}}{l} (c_2 \ddot{\psi} + v \dot{\psi}) - \\ & - \frac{J_{2UV}}{l} (c_1 \ddot{\psi} + v \dot{\psi}) - \frac{1}{l} [(c_1 N_2 + c_2 N_1) \dot{\psi} + \\ & + (N_1 + N_2) v \psi] - \frac{v}{l} [(m_1 h_1 c_2 + m_2 h_2 c_1) \dot{\psi} + \\ & + (m_1 h_1 + m_2 h_2) v \psi] - g [m_1 h_1 \vartheta_1 + m_2 h_2 \vartheta_2 - \\ & - \left(m_2 \frac{r_2}{l} - m_1 \frac{r_1}{l} \right) (c_1 - r) \psi] = 0 \end{aligned} \right\} (30)$$

and according to Eq. (24) we get for rotation about the steering axis

$$\begin{aligned} & \left[\frac{c_2^2}{l} (J_{1V} \cos \sigma + J_{1UV} \sin \sigma) + \right. \\ & \left. + \frac{c_1^2}{l} (J_{2V} \cos \sigma + J_{2UV} \sin \sigma) \right] \ddot{\psi} - \\ & - c_2 (J_{1UV} \cos \sigma + J_{1U} \sin \sigma) \ddot{\vartheta}_1 - \\ & - c_1 (J_{2UV} \cos \sigma + J_{2U} \sin \sigma) \ddot{\vartheta}_2 + \\ & + \left[\frac{c_2^2}{l} (J_{1V} \cos \sigma + J_{1UV} \sin \sigma) + \right. \\ & \left. + \frac{c_1^2}{l} (J_{2V} \cos \sigma + J_{2UV} \sin \sigma) \right] v \dot{\psi} + \end{aligned}$$

$$\begin{aligned}
 & + (c_2 N_1 \dot{\theta}_1 + c_1 N_2 \dot{\theta}_2) \cos \sigma + \frac{1}{l} (N_2 c_1^2 + N_1 c_2^2) \dot{\psi} \sin \sigma + \\
 & + \frac{v}{l} (c_2 N_1 + c_1 N_2) \psi \sin \sigma + \frac{v}{l} (c_2^2 m_1 s_1 + c_1^2 m_2 s_2) \dot{\psi} + \\
 & + \frac{v^2}{l} (c_2 m_1 s_1 + c_1 m_2 s_2) \psi + g (c_2 m_1 s_1 \theta_1 + c_1 m_2 s_2 \theta_2) - \\
 & - g c_1 c_2 \left(m_2 \frac{r_2}{l} - m_1 \frac{r_1}{l} \right) \psi \sin \sigma - (c_1 - c_2) M_D = 0
 \end{aligned}$$

..... (31).

Eq. (31) contains the essential terms which cause steering deflection. Thus on the left side of the equation the two terms with the factor $c_1 v \dot{\psi} / l$ (eleventh and twelfth summand) take into account the driving forces which the frame system exerts on the hinged part. A pressure in the plane of the frame and acting on the hinged system obviously causes the front wheel to turn into the plane of the frame (like the pulled wheel of a wagon). The next six terms (with N_1 and N_2) give the gyroscopic action which are due to a steering deflection or rolling of the machine. The four following terms (with $v \dot{\psi} / l$ and $v^2 \psi / l$) take into account the centrifugal forces. The next two terms are for the moment due to gravity which seeks to rotate the handlebar and the frame about the steering axis when the motorcycle is tilted, hence the static steering forces. The following two terms (with $g \psi$) correspond to the drop in c.g. position (which has already been mentioned) when the handlebar is deflected, and the last terms with M_D include the effect of a friction steering damper.

With the aid of the kinematic relationship, Eq. (29), it would be possible to reduce the three angular coordinates θ_1 , θ_2 and ψ contained in Eq. (30) and (31) to two. For the purposes of calculation, however, it is simpler to add the kinematic relationship as a third condition equation.

1.9 Solution of the Equations of Motion

Setting

$$\theta_1 = C_1 e^{\lambda t}, \quad \theta_2 = C_2 e^{\lambda t}, \quad \psi = C_3 e^{\lambda t} \dots (32)$$

where t is the time, λ a frequency parameter and C_1, C_2, C_3 , are constants, we get from Eq. (29) to (31) the linear equations for determining C_1, C_2 , and C_3

$$C_1 - C_2 + C_3 \operatorname{tg} \sigma = 0 \dots \dots \dots (33)$$

$$\left. \begin{aligned}
 & C_1 (J_{1U} \lambda^2 - g m_1 h_1) + C_2 (J_{2U} \lambda^2 - g m_2 h_2) + \\
 & + C_3 \left\{ -\frac{J_{1UV}}{l} (c_2 \lambda^2 + v \lambda) - \frac{J_{2UV}}{l} (c_1 \lambda^2 + v \lambda) - \right. \\
 & - \frac{\lambda}{l} (c_1 N_2 + c_2 N_1) - \frac{v}{l} (N_1 + N_2) - \\
 & - \frac{v}{l} [\lambda (m_1 h_1 c_2 + m_2 h_2 c_1) + v (m_1 h_1 + m_2 h_2)] + \\
 & \left. + g \left(m_2 \frac{r_2}{l} - m_1 \frac{r_1}{l} \right) (c_1 - c_2) \right\} = 0
 \end{aligned} \right\} (34)$$

$$\begin{aligned}
 & C_1 [-c_2 \lambda^2 (J_{1UV} \cos \sigma + J_{1U} \sin \sigma) + c_2 N_1 \lambda \cos \sigma + g c_2 m_1 s_1] + \\
 & + C_2 [-c_1 \lambda^2 (J_{2UV} \cos \sigma + J_{2U} \sin \sigma) + c_1 N_2 \lambda \cos \sigma + g c_1 m_2 s_2] + \\
 & + C_3 \left\{ \lambda^2 \left[\frac{c_2^2}{l} (J_{1V} \cos \sigma + J_{1UV} \sin \sigma) + \frac{c_1^2}{l} (J_{2V} \cos \sigma + J_{2UV} \sin \sigma) \right] + \lambda v \left[\frac{c_2}{l} (J_{1V} \cos \sigma + J_{1UV} \sin \sigma) + \right. \right. \\
 & \left. \left. + \frac{c_1}{l} (J_{2V} \cos \sigma + J_{2UV} \sin \sigma) \right] + \frac{\lambda}{l} (N_2 c_1^2 + N_1 c_2^2) \sin \sigma + \frac{v}{l} (c_2 N_1 + c_1 N_2) \sin \sigma + \right. \\
 & \left. + \frac{\lambda v}{l} (c_2^2 m_1 s_1 + c_1^2 m_2 s_2) + \frac{v^2}{l} (c_2 m_1 s_1 + c_1 m_2 s_2) - g c_1 c_2 \left(m_2 \frac{r_2}{l} - m_1 \frac{r_1}{l} \right) \sin \sigma \right\} = (c_1 - c_2) M_D
 \end{aligned} \tag{35}$$

Eq. (35) is not homogeneous since the constant frictional damping occurs in it. To begin with, however, the damping will be set equal to zero, i.e. the motion is considered without the use of the steering damper.

Eq. (33) to (35) are now non-dimensionalized by introducing a reduced frequency Ω and a reduced time τ defined by

$$\Omega = \lambda l / v, \quad \tau = v t / l \dots \dots \dots \tag{36}$$

In this way, insertion of numerical values gives information concerning not just one machine, but all machines with the same relationships of masses, inertias, lengths, and gyroscopic terms. Since the system moves under the influence of gravity, the Froude Number $Fr = v / \sqrt{g l}$ occurs in the equations.

The following abbreviations and ratios will be used in further calculations:

$$\begin{aligned}
 f &= 1 / Fr^2 = g l / v^2, \\
 M &= m_1 / m_2 \quad \text{as mass ratio} \\
 K_{1U} &= k_{1U} / l, \quad K_{1V} = k_{1V} / l, \quad K_{1UV} = k_{1UV} / l, \\
 K_{2U} &= k_{2U} / l, \quad K_{2V} = k_{2V} / l, \quad K_{2UV} = k_{2UV} / l
 \end{aligned}$$

as inertia ratios (with $k = \sqrt{J/m}$ as radius of gyration, $J = J_{1U}, J_{1V}, J_{1UV}, J_{2U}, J_{2V}$ or J_{2UV} , $m = m_1$ or m_2 , subscript 1 and 2 for the front and rear wheel system, respectively, subscript U and V values which come from the moment of inertia about the U and V axes, respectively, subscript UV for values which come from the centrifugal moment in the UV plane). The two wheels have the same moment of inertia J_1 , but according to Section 1.4 the moment of inertia of the motor J_{mot} is to be added to that of the rear wheel; thus $J_2 = J_1 + J_{mot}$. The calculation is simplest if the radius of gyration $k_R = \sqrt{J_1 / m_{1R}}$ of the wheel without the motor is retained with m_{1R} as reduced mass of the front wheel (i.e. of the wheel alone) and a reduced mass m_{2R} is introduced for the rear wheel with the motor; this amounts to

$$m_{2R} = (J_1 + J_{mot}) / k_{1R}^2 = J_2 / k_R^2$$

In the dimensionless representation, the following additional notation is introduced:

$$M_{1k} = m_{1R}/m_2, \quad M_{2k} = m_{2R}/m_2$$

as gyroscopic mass ratio of the two systems, $K_R = k_R/\sqrt{I}R$ as gyroscopic inertia ratio with R as the effective radius which is the same for both wheels and

$$H_1 = h_1/l, \quad H_2 = h_2/l, \quad C_1^* = c_1/l, \quad C_2^* = c_2/l, \\ R_1^* = r_1/l, \quad R_2^* = r_2/l, \quad R^* = r/l, \quad S_1 = s_1/l, \quad S_2 = s_2/l$$

as length ratios. Further, from Eq. (14)

$$N_1 = m_{1R} k_R^2 \nu / R, \quad N_2 = m_{2R} k_R^2 \nu / R.$$

While Eq. (33) remains unchanged, Eq. (34) and (35) now go over into

$$\alpha_{11} C_1 + \alpha_{12} C_2 + \alpha_{13} C_3 = 0 \dots \dots \dots (37)$$

and for $M_D = 0$ correspondingly

$$\alpha_{21} C_1 + \alpha_{22} C_2 + \alpha_{23} C_3 = 0 \dots \dots \dots (38)$$

with

$$\alpha_{11} = M (K_{1U}^2 \Omega^2 - I H_1), \\ \alpha_{12} = K_{2U}^2 \Omega^2 - I H_2, \\ \alpha_{13} = -M K_{1UV}^2 \Omega (C_2^* \Omega + 1) - K_{2UV}^2 \Omega (C_1^* \Omega + 1) - \\ - \Omega K_{1R}^2 (C_1^* M_{2k} + C_2^* M_{1k}) - K_R^2 (M_{1k} + M_{2k}) - \\ - \Omega (C_2^* H_1 M + C_1^* H_2) - (M H_1 + H_2) + \\ + f (R_2^* - M R_1^*) (C_1^* - R^*), \\ \alpha_{21} = -\Omega^2 C_2^* M (K_{1U}^2 \sin \sigma + K_{1UV}^2 \cos \sigma) + \\ + \Omega C_2^* M_{1k} K_R^2 \cos \sigma + f M C_2^* S_1, \\ \alpha_{22} = -\Omega^2 C_1^* (K_{2U}^2 \sin \sigma + K_{2UV}^2 \cos \sigma) + \\ + \Omega C_1^* M_{2k} K_R^2 \cos \sigma + f C_1^* S_2 \quad \text{and} \\ \alpha_{23} = \Omega^2 [C_2^{*2} M (K_{1V}^2 \cos \sigma + K_{1UV}^2 \sin \sigma) + \\ + C_1^{*2} (K_{2V}^2 \cos \sigma + K_{2UV}^2 \sin \sigma)] + \Omega [C_2^* M (K_{1V}^2 \cos \sigma + \\ + K_{1UV}^2 \sin \sigma) + C_1^* (K_{2V}^2 \cos \sigma + K_{2UV}^2 \sin \sigma) + \\ + K_R^2 \sin \sigma (C_1^{*2} M_{2k} + C_2^{*2} M_{1k})] + \\ + K_R^2 \sin \sigma (C_2^* M_{1k} + C_1^* M_{2k}) + \Omega (M C_2^{*2} S_1 + C_1^{*2} S_2) + \\ + M C_2^* S_1 + C_1^* S_2 - f C_1^* C_2^* (R_2^* - M R_1^*) \sin \sigma.$$

The system of the three equations, Eq. (33), (37) and (38), which are now homogeneous and linear, has solutions only if the coefficient determinant vanishes

$$\Delta \begin{vmatrix} \alpha_{11} & \alpha_{12} & \alpha_{13} \\ \alpha_{21} & \alpha_{22} & \alpha_{23} \\ 1 & -1 & t_g \sigma \end{vmatrix} = 0 \quad \dots \dots (39)$$

This requirement gives a fourth degree equation for Ω because the sum of the orders of the differential equations is equal to 4. Thus the system has two oscillations. They are stable if all four roots have complex values with negative real parts. In this case there are two damped oscillations. On the other hand, if two real roots occur, then the motion is stable if they are negative.

Evaluation of the coefficient determinant leads to an equation for Ω of the form

$$\left. \begin{aligned} \varepsilon_4 \Omega^4 + \varepsilon_3 \Omega^3 + (\varepsilon_{21} - \varepsilon_{22} f) \Omega^2 + \\ + (\varepsilon_{11} - \varepsilon_{12} f) \Omega + (\varepsilon_{01} f - \varepsilon_{02}) f = 0 \end{aligned} \right\} \dots \dots (40)$$

with the ε values as constants of the vehicle. Explicit expression of the roots of this algebraic equation of fourth degree as functions of f is not possible in practice. Hence numerical calculation must begin with the determinant. For this purpose, the dimensions of the motorcycle and its moments of inertia must be determined.

2. Applications

2.1 Calculation of the Natural Oscillations of Test Machines

The moments of inertia of the front wheel system and of the wheels of some machines were determined with the aid of a bifilar suspension; the moments of inertia of the frame with rider were determined by suspending them about the individual axes of rotation on an oscillating turntable. The investigations were carried out on three typical single-track vehicles: a scooter (Vespa), a light motorcycle (Dürkopp MD 150) and a heavy motorcycle (BMW R 51/3) with and without passenger. Fig. 4 to 6 show the inertia ellipsoids of these machines in the plane of the wheels; Table 1 contains the basic quantities.

These basic quantities must now be substituted into the coefficient determinant, Eq. (39). The fourth degree equations (for the four roots Ω_1 to Ω_4 of Ω) which result when Eq. (39) is expanded out contain f as a parameter. They are

$$\begin{aligned} \Omega^4 + 18,9 \Omega^3 + (16,7 - 17,6 f) \Omega^2 + (6,79 - 12,8 f) \Omega + \\ + (1,64 f - 1,53) f = 0, \end{aligned}$$

for the Vespa scooter,

$$\Omega^4 + 3,9\Omega^3 + (4,65 - 6,75f)\Omega^2 + (3,38 - 4,74f)\Omega + (6,34f - 1,32)f = 0,$$

for the Dürkopp machine, Type MD 150,

$$\Omega^4 + 4\Omega^3 + (5,59 - 5,61f)\Omega^2 + (3,08 - 3,84f)\Omega + (6,02f - 1,05)f = 0$$

for the BMW machine, Type R 51/3 with driver alone, and

$$\Omega^4 + 4,48\Omega^3 + (5,76 - 5,68f)\Omega^2 + (2,36 - 3,59f)\Omega + (5,44f - 0,803)f = 0.$$

with passenger. After f was substituted, the roots of Ω were determined by iteration and collected in Table 2. In all cases there were two real and two complex roots. It can be seen that complete stability occurs only in the small region from $v \approx 20$ to 30 km/hr for the motorcycles and $v \approx 30$ to 40 km/hr for the scooter.

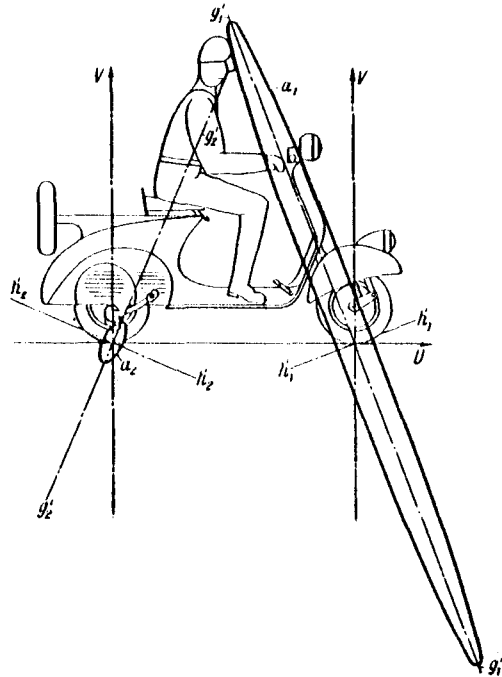


Fig. 4

Inertia ellipsoids of the Vespa scooter in the plane of the wheels U and V space-fixed coordinate system, a_1 and a_2 ellipsoid of the front and rear wheel systems, resp. with principal axes $g'_1 - g'_1$ and $h'_1 - h'_1$, and $g'_2 - g'_2$ and $h'_2 - h'_2$ respectively

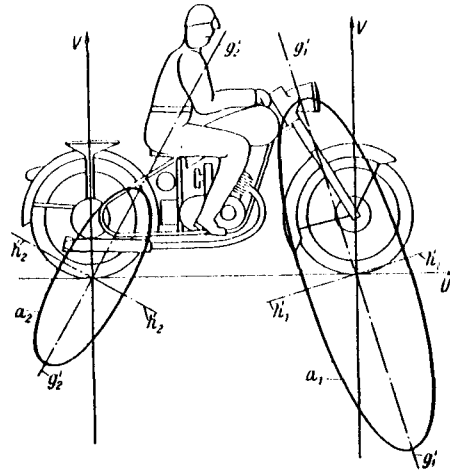


Fig. 5
Inertia ellipsoids of the Dürkopp MD 150 machine in the plane of the wheels
Notation as in Fig. 4

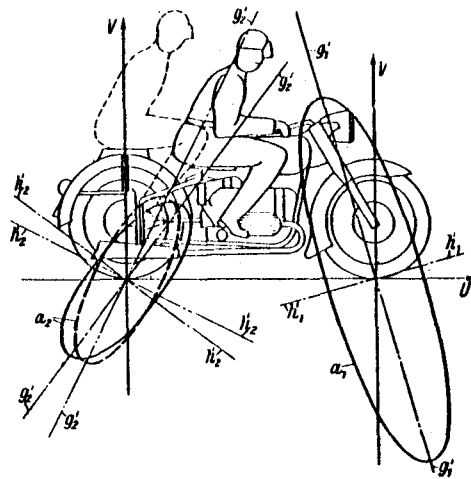


Fig. 6
Inertia ellipsoids of the BMW R 51/3 machine in the plane of the wheels
Notation as in Fig. 4, solid lines for solo operation;
dashed curve a_2 holds for operation with passenger (dashed)

We now insert the four roots Ω_1 to Ω_4 into Eq. (33), (37) and (38) and determine C_1 to C_3 . Ω_1 gives C_{11} , C_{21} and C_{31} ; Ω_2 gives C_{12} , C_{22} and C_{23} etc. Using the expressions of Eq. (32) and adding gives

$$\begin{aligned} \dot{\varphi}_1 = & A C_{11} e^{\Omega_1 \tau} + B C_{12} e^{\Omega_2 \tau} + C C_{13} e^{\Omega_3 \tau} + \\ & + D C_{14} e^{\Omega_4 \tau} \end{aligned} \quad \dots (41),$$

$$\begin{aligned} \dot{\varphi}_2 = & A C_{21} e^{\Omega_1 \tau} + B C_{22} e^{\Omega_2 \tau} + C C_{23} e^{\Omega_3 \tau} + \\ & + D C_{24} e^{\Omega_4 \tau} \end{aligned} \quad \dots (42),$$

$$\begin{aligned} \psi = & A C_{31} e^{\Omega_1 \tau} + B C_{32} e^{\Omega_2 \tau} + C C_{33} e^{\Omega_3 \tau} + \\ & + D C_{34} e^{\Omega_4 \tau} \end{aligned} \quad \dots (43).$$

Table 1. Basic Parameters of the Test Machines

Notation			Vespa Scooter	Dürkopp MD 150	BMW R 51/3 Solo	BMW R 51/3 with passenger
Mass of the front wheel system	m_1	kg s ² /cm	0.011424	0.02242	0.03711	0.03711
Height of c.g. of front wheel system	h_1	cm	36.3	49.3	54.2	54.2
Horizontal distance of c.g. from point of contact (front wheel)	r_1	cm	7.0	11.4	13.2	13.2
Castor trail	c_1	cm	8.5	10.5	8	8
Distance of c.g. from line parallel to steering axis and through point of contact (front wheel)	s_1	cm	4.44	12.6	12.7	12.7
Moment of inertia about V axis (front wheel)	J_{1V}	kg cm s ²	4	11.6	20.2	20.2
Moment of inertia about U axis (front wheel)	J_{1U}	kg cm s ²	28	69	135	135
Product of inertia in UV plane (front wheel)	J_{1UV}	kg cm s ²	-10.5	-18.1	-36.4	-36.4
Moment of inertia of front wheel about wheel axis	J_1	kg cm s ²	0.84	4.6	6.5	6.5
Mass of rear wheel system	m_2	kg s ² /cm	0.1588	0.1464	0.2161	0.2861
Height of c.g. of rear wheel system	h_2	cm	60.2	70.2	55.0	62.9
Horizontal distance of c.g. from point of contact (rear wheel)	r_2	cm	31.3	43.3	52.4	44.1
Distance of intersection point of steering axis from rear point of contact	c_2	cm	125.8	139.5	151	151
Distance of c.g. from steering axis (rear wheel)	s_2	cm	48.3	70.8	71.8	68.0
Moment of inertia about V axis (rear wheel)	J_{2V}	kg cm s ²	340	360	720	720
Moment of inertia about U axis (rear wheel)	J_{2U}	kg cm s ²	1210	850	1110	2100
Product of inertia in UV plane (rear wheel)	J_{2UV}	kg cm s ²	440	400	670	850
Moment of inertia of rear wheel and motor	J_2	kg cm s ²	1.5	6.0	6.5	6.5
Wheelbase	l	cm	117.3	129.0	143	143
Effective wheel radius	R	cm	17.8	30.7	32.4	32.4
Rake angle	σ	Grad	21	27.5	26.9	26.9
Horizontal distance of point of application of reaction forces from point of contact	r	cm	2.41	5.43	6.46	5.56
Radius of gyration of the wheel	k_R	cm	14.2	21.2	23	23
Mass of front wheel	m_{1R}	kg s ² /cm	0.00415	0.0102	0.0125	0.0125
Reduced mass of rear wheel with motor	m_{2R}	kg s ² /cm	0.0074	0.0133	0.0125	0.0125

The four constants, A, B, C, D were introduced in order to satisfy the initial conditions $\theta_1 = \theta_1(0)$, $\dot{\theta}_1 = d\theta_1/d\tau = \dot{\theta}_1(0)$, $\psi = \psi(0)$ and $\dot{\psi} = d\psi/d\tau = \dot{\psi}(0)$ for $\tau = 0$. The kinematic condition, Eq. (29), gives the roll angle θ_2 in terms of θ_1 and ψ .

At a speed of $v = 90$ km/hr, for example, the equation for the roll angle of the frame of the Vespa scooter is

$$\vartheta_2 = A C_{21} e^{-0,46\tau + 0,41\tau} + B C_{22} e^{-0,46\tau - 0,41\tau} + \left. \begin{aligned} &+ C C_{23} e^{-18,1\tau} + D C_{24} e^{0,0047\tau} \end{aligned} \right\} (44)$$

or

$$\vartheta_2 = e^{-0,46\tau} \left[(A C_{21} + B C_{22}) \cos(0,4\tau) + \right. \\ \left. + (A C_{21} - B C_{22}) i \sin(0,4\tau) \right] + C C_{23} e^{-18,1\tau} + \left. \begin{aligned} &+ D C_{24} e^{0,0047\tau} \end{aligned} \right\} (45)$$

The motion is thus composed of three basic components: a damped oscillation, a term which goes to zero very rapidly with time, and a slowly increasing term.

2.2 The Amplitude Ratio

From Eq. (32) we can form the amplitude ratio of the roll angle of the frame to the steering deflection (measured on the ground):

$$C_2/C_3 = \vartheta_2/\psi \dots \dots \dots (46)$$

If C_1 is substituted into Eq. (37) from Eq. (33), it follows that

$$C_2/C_3 = -(\alpha_{13} - \alpha_{11} \operatorname{tg} \sigma) / (\alpha_{11} + \alpha_{12}) \dots \dots (47).$$

When numerical values are substituted, equations result in which the parameter f and $\Omega(f)$ still occur, as for example, for the Vespa scooter:

$$\frac{C_2}{C_3} = \frac{-1,45 \cdot 10^{-2} \Omega^2 - 2,82 \cdot 10^{-1} \Omega - 5,48 \cdot 10^{-1} + 3,04 \cdot 10^{-2} f}{5,64 \cdot 10^{-1} \Omega^2 - 5,41 \cdot 10^{-1} f}$$

For complex values $\Omega_1 = -\alpha + i\beta$ and $\Omega_2 = -\alpha - i\beta$ we also get complex amplitude ratios of the form

$$C_2/C_3 = -E + iF \dots \dots \dots (48)$$

If, for example, we choose $AC_{31} = 1$ and $BC_{32} = 0$ in Eq. (43) so that Ω_1 determines the oscillation, then the motion of the steering deflection, which takes the form of a damped oscillation, is given by

$$\psi = e^{(-\alpha + i\beta)\tau} = e^{-\alpha\tau} [\cos(\beta\tau) + i \sin(\beta\tau)] \quad (49)$$

Table 2. Roots of Reduced Frequency Ω

Froude Number Fr	Speed		Ω_1 and Ω_2	Roots Ω_3	Ω_4
	km/hr	cm/sec			
Vespa Scooter					
7.37	90	2.5×10^3	$-0.46 \pm 0.4 i$	-18.1	0.0047
4.9	60	1.67×10^3	$-0.45 \pm 0.4 i$	-18.1	0.0056
3.27	39.92	1.109×10^3	$-0.41 \pm 0.37 i$	-18.2	0
2.46	30	8.33×10^2	$-0.35 \pm 0.31 i$	-18.1	-0.049
1.64	20	5.55×10^2	$0.037 \pm 0.38 i$	-18.4	-0.0625
0.82	10	2.78×10^2	$0.85 \pm 0.82 i$	-19.4	-0.125
Dürkopp Machine Type MD 150					
7.03	90	2.5×10^3	$-0.6 \pm 0.91 i$	-2.7	0.006
4.7	60	1.67×10^3	$-0.57 \pm 0.895 i$	-2.76	0.012
2.34	30	8.33×10^2	$-0.48 \pm 0.82 i$	-3.15	0
1.56	20	5.55×10^2	$0.038 \pm 0.62 i$	-3.5	-0.49
0.786	10	2.78×10^2	$1.24 \pm 0.76 i$	-4.0	-1.46
BMW Machine, Type R 51/3, Solo					
8.9	120	3.33×10^3	$-0.95 \pm 0.74 i$	-2.11	0.0041
6.68	90	2.5×10^3	$-0.93 \pm 0.74 i$	-2.15	0.0068
4.45	60	1.667×10^3	$-0.88 \pm 0.735 i$	-2.26	0.013
2.4	32.3	8.97×10^2	$-0.69 \pm 0.67 i$	-2.65	0
1.85	25	6.941×10^2	$-0.49 \pm 0.53 i$	-2.9	-0.136
1.12	15.09	4.19×10^2	$0.41 \pm 0.74 i$	-3.65	-1.15
BMW Machine, Type R 51/3 with Passenger					
8.9	120	3.33×10^3	$-0.9 \pm 0.24 i$	-2.68	0.004
6.68	90	2.5×10^3	$-0.9 \pm 0.27 i$	-2.72	0.0066
4.45	60	1.667×10^3	$-0.85 \pm 0.31 i$	-2.82	0.0012
2.6	35.09	9.742×10^2	$-0.7 \pm 0.23 i$	-3.08	0
1.85	25	6.941×10^2	$-0.2 \pm 0.24 i$	-3.38	-0.72
1.12	15	4.167×10^2	$0.45 \pm 0.65 i$	-4.57	-0.97

The roll angle of the frame is then given by

$$\theta_2 = (-E + iF)\psi \dots \dots \dots (50).$$

from Eq. (42) with ψ from Eq. (49). If the oscillation of the steering system is represented as a rotating vector in the Gaussian plane, Fig. 7, then this vector must be multiplied by $(-E + iF)$; this gives a second vector for the corresponding oscillation of the frame system about the track.

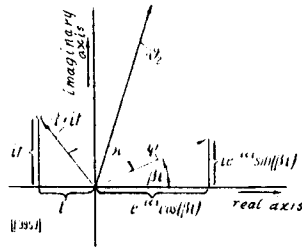


Fig. 7
Representation of the angles θ_2 and ψ and the amplitude ratio $-E + iF$ in the Gaussian plane
Explanations in text

As can be seen from Fig. 7, the phase of the roll angle (i.e. the angle θ_2) is shifted with respect to the steering oscillation (determined by the angle ψ) by an angle κ which is given by

$$\text{tg } \kappa = F/E \dots \dots \dots (51)$$

The quantity $\sqrt{E^2 + F^2}$ gives the ratio of the peak values; this is the amount by which the vector representing the rolling oscillation is greater than the steering oscillation set equal to 1. The two real roots Ω_3 and Ω_4 give real amplitude ratios. Fig. 8 to 11 show the amplitude ratio θ_2/ψ and the phase shift in the Gaussian plane for the test machines, normalized to $\psi = 1$.

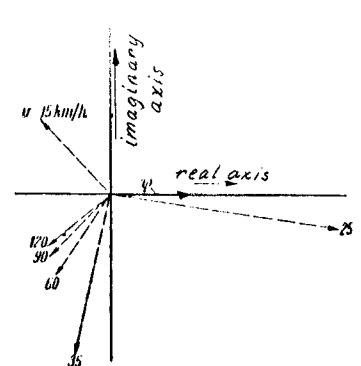
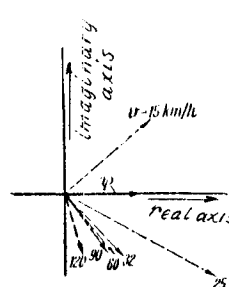
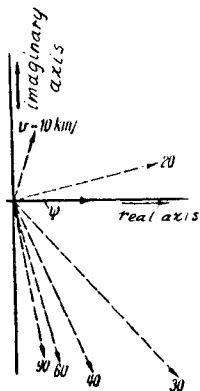


Fig. 8. Amplitude ratio θ_2/ψ for the Vespa scooter for various speeds v . Dashed vectors for θ_2/ψ with $\psi = 1$

Fig. 9. Amplitude ratio θ_2/ψ for the Dürkopp MD 150 machine for various speeds v . Explanation as in Fig. 8

Fig. 10. Amplitude ratio θ_2/ψ for the BMW R 51/3 machine, solo, for various speeds v . Explanation as in Fig. 8

Fig. 11. Amplitude ratio θ_2/ψ for the BMW R 51/3 machine with passenger for various speeds v . Explanation as in Fig. 8

2.3 The Motion

By means of the above results the motion of single-track vehicles in the neighborhood of the equilibrium condition without interference by the driver will be considered. Three characteristic types of motion occur: the complex values Ω_1 and Ω_2 represent an oscillation, the negative real root Ω_3 requires a very rapid decrease in deflection and the small positive root Ω_4 gives rise to a slow increase of the deflection (or for low speeds, when Ω_4 is also negative, a decrease in the initial deflection).

It is useful to distinguish three speed ranges. In the first range the motion is unstable. For very low speeds (1 to 5 km/hr) there are two positive real roots instead of the complex ones. Left to themselves, therefore, both systems collapse because of gravity. Numerical values were not determined in this regime. For somewhat higher speeds the two complex roots have positive real parts; an increasing oscillation is thus set up. At first the real part of the roots is so large that no periodic motion can exist. As the speed increases, the real part gets smaller and smaller, and more and more of an oscillation arises. For a speed which is between 15 to 30 km/hr for the common single-track vehicles of today, the damping factor which has been positive and which was the source of instability at the lowest speeds passes through zero and begins to take on negative values. This is the boundary to the next speed range.

In the lowest speed range the two real roots are negative. In the higher speed range the negative value for Ω_3 remains practically constant. After some disturbance the recovery with an absolute value of the frequency $\lambda = \Omega_3 v/\ell$ according to Eq. (36) therefore takes place more rapidly as the speed increases. The small negative root Ω_4 moves closer and closer to zero with increasing speed, and, for common vehicles, reaches it at speeds of 32 to 42 km/hr. In the second velocity range, therefore, the motion is stable in the neighborhood of equilibrium.

The middle speed range ends when the small root Ω_4 passes through zero, since from now on this root takes on small positive values. They indicate a slow tipping of the motorcycle. As a matter of fact, at still higher speeds these positive values again get somewhat smaller; but they never return to zero. The damping factor (real part of Ω_1 and Ω_2) and the dimensionless frequency (imaginary part of Ω_1 and Ω_2) are approximately constant in the upper speed range of about 50 km/hr ($Fr \approx 4$). The corresponding absolute magnitudes thus again increase linearly with speed (cf. Eq. (36)). Whence it follows that the wave length L in the track

$$L = (2\pi/\nu) v \dots \dots \dots (52)$$

where ν is the absolute frequency (imaginary part of $\lambda = \Omega v/\ell$) remains constant for speeds of more than 50 km/hr.

If the tires of the motorcycle were painted with stamp pad ink, the machine would always leave the same pattern of oscillations on the road in the upper speed range, regardless of whether, as an example, $v = 60$ km/hr or 260 km/hr. Even though the instability is small in the third speed range, it is nevertheless somewhat surprising at first because it is our experience that it is particularly easy to ride no-handed at higher speeds. However, once he is made aware of the fact, every driver perceives very clearly how he must shift his weight from one side to the other when driving no-handed with $v \geq 40$ km/hr because the machine slowly tilts. Corresponding to the very slow increase in deflection, this compensation takes place in about 4 to 10 seconds.

The small positive root Ω_4 , the expression of the instability, arises from the fact that the factor $(\epsilon_{01} f - \epsilon_{02}) f$ in Eq. (40) takes on negative values as the speed

v increases (hence as f decreases) because of the negative sign of ε_{02} . In the equation of motion, Eq. (31), the term $\varepsilon_{02} f$ corresponds to terms with the factor $v^2 \psi$. But these terms first arose from the introduction of the relation $\varphi_1 - \varphi_2 = \psi$ and the non-holonomic Eq. (4). Clearly this means that, during the motion, after a steering deflection the rear wheel again approaches the track of the front wheel, since it is hinged at an axis in the plane of the front wheel, and so angle ψ continually decreases. If, after a steering deflection, the front wheel moves along a straight line, then the rear wheel moves along a tractrix asymptotically toward the track of the front wheel. The greater the speed, the more rapidly this approach and hence the decrease of ψ takes place. If we let $v = \infty$, then from Eq. (4) with $\varphi_1 - \varphi_2 = \psi$ we have the angle $\psi = 0$ inasmuch as the angular velocities $\dot{\varphi}_1$ and $\dot{\varphi}_2$ remain finite. With $\psi = 0$, however, there would be no possibility of a steering deflection on which the stabilization naturally depends.

It should still be mentioned that for smaller σ , i.e. steeper rake angle, this instability may be reduced and even entirely eliminated (in this case the last term of Eq. (40) becomes $(\varepsilon_{01} f + \varepsilon_{02}) f$). However, this measure also decreases the damping factor of the complex roots which, because of the danger of steering shimmy, is much more important than the small, completely harmless instability in the upper velocity range.

With the aid of the amplitude ratio we can recognize the part of the roll angle and the steering deflection due to the three characteristic motions. The part of the rolling motion due to the recovery determined by Ω_3 becomes vanishingly small at high speeds; it gets larger with decreasing v . This rapid motion is carried out almost exclusively by the lighter front wheel system as a result of a control deflection. Conversely the behavior of the motorcycle during the slow rolling motion is due to the small value of Ω_4 . Here the rolling motion of the frame system gives rise to the displacement; the steering deflection takes part in the motion practically only at the lower speeds. Finally the phase shift (of the oscillatory motion) determined by the complex amplitude ratio must be considered. In the lowest speed range the roll attitude leads the steering deflection. In the middle speed range, however, the roll attitude begins (between 20 to 30 km/hr) to lag behind the steering deflection, and with increasing velocity it lags more and more. The amplitude ratio reaches a maximum value at 25 to 30 km/hr. With increasing speed it becomes somewhat smaller; and with decreasing speed it becomes considerably smaller. At its maximum value, the amplitude of the roll attitude is 2 to 3 times that of the steering deflection.

2.4 Comparison of Test Machines

To compare the results for the individual test machines, the roots Ω_1 to Ω_4 have been graphed as functions of the Froude Number Fr , Fig. 12 to 15. It should be noted that all the curves are nearly constant in the upper speed range. The most important quantities are the frequency and the damping factor since oscillation phenomena are the major source of danger at high speeds. For the Vespa scooter the damping factor (cf. Fig. 12) has the smallest absolute value; then come the Dürkopp MD 150 machine and, with a considerably larger absolute value of damping, the BMW R 51/3 machine with driver alone. The passenger, in the case of the heavier machine, causes only a slight decrease in the absolute value of the damping factor. Without a doubt, a maximum possible absolute value of the damping factor is desirable and should be the object of the layout of the mechanism. However, this alone does not suffice to insure good riding characteristics because it is precisely in machines with maximum damping that tendencies toward shimmy have been observed and measured.

The natural frequency of the oscillations (cf. Fig. 13) is highest for the Dürkopp machine. Gyroscopic forces which are large relative to the vehicle mass are the reason for this. The frequency of the BMW R 51/3 machine with driver only has final values about 27% smaller, while the frequency of the Vespa scooter is only half that of the Dürkopp machine. With a passenger the frequency of the BMW machine decreases by more than half

that of the solo-machine. For lighter machines a still greater decrease in frequency can be expected when a passenger is added. In any case, the difference is not so great in practice because the passenger, due to his peculiar inability to remain fixed, is not "rigidly attached to the machine" during all its motions; actually the mass of the machine is increased by only part of his mass. Measurements have shown that the frequency actually decreases by only about 10% with a passenger.

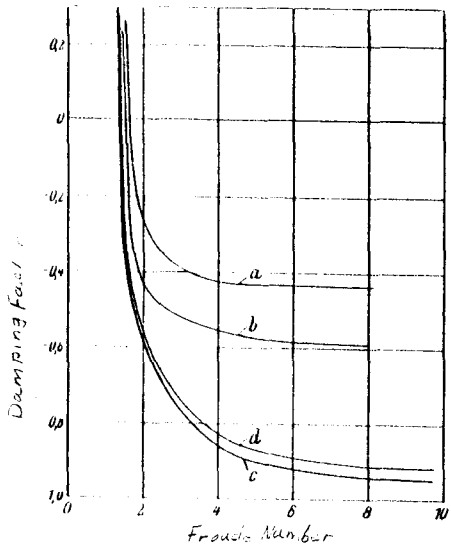


Fig. 12. Damping factor (real part of the roots Ω_1 and Ω_2) of the oscillation vs. Froude Number
 a Vespa scooter, b Dürkopp MD 150 machine, c BMW R 51/3 machine, solo, d BMW R 51/3 machine with passenger

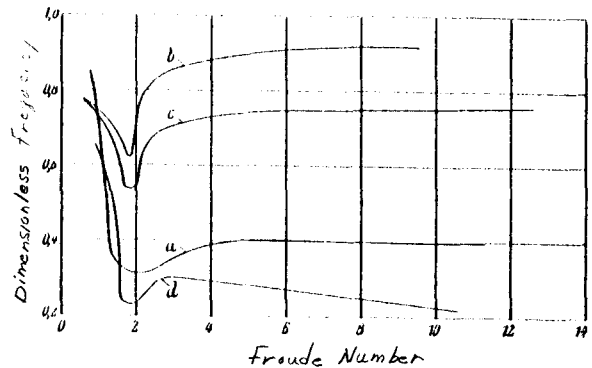


Fig. 13. Dimensionless frequency (imaginary part of the roots Ω_1 and Ω_2) of the oscillation as a function of Froude Number
 Explanations as in Fig. 12

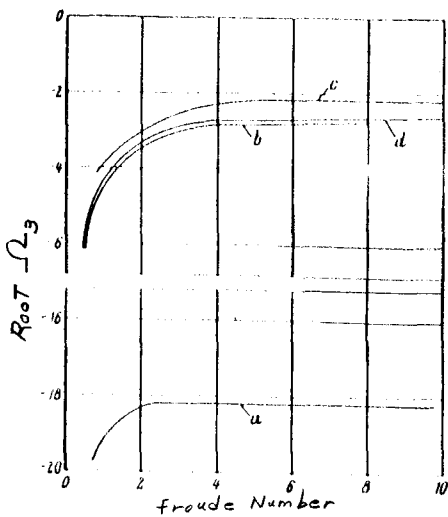


Fig. 14. Root Ω_3 for return to null position as a function of Froude Number
 Explanations as in Fig. 12

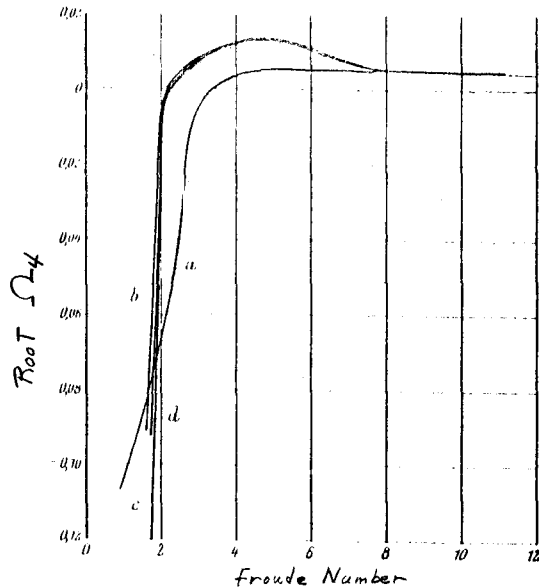


Fig. 15. Root Ω_4 for the slow increase of deflection at high speeds as a function of Froude Number
 Explanations as in Fig. 12

The value of the negative roots Ω_3 , which determine the restoration after a disturbance deflection, differ only slightly for the motorcycles (cf. Fig. 14). The absolute value for the Vespa scooter, however, is 7 to 8 times the values for the motorcycles (because of the small mass of the hinged part).

The root Ω_4 is of most interest in the upper speed range. With increasing speed the values for the motorcycles approach one another and are about equal beyond $Fr = 8$ (corresponding to $v \approx 60$ km/hr). Beyond about $Fr \approx 2$ the curve for Ω_4 of the scooter falls somewhat below the other curves, but as the speed increases it approaches the values for the motorcycles.

For operating conditions the roots Ω_3 and Ω_4 have no great significance and hence are unimportant in the design of vehicles. The small instability due to Ω_4 is readily corrected by the driver, for the slow increase in deflection, with no additional effort. The restoring action of the hinged part corresponding to Ω_3 is a desirable motion. On the other hand particular attention must be paid to the oscillation frequency; it must not be in the vicinity of the natural frequency of any system of the machine which is subject to oscillation, and must also not be in the range of frequencies associated with oscillations due to road roughness because otherwise oscillations arising from strong damping can occur.

2.5 The Action of the Steering Damper

The tendency to shimmy is generally suppressed by a friction damper which can be applied when needed by the driver at higher speeds and has the usual effect of friction damping on an oscillating system. The damper decreases the amplitude linearly without changing the frequency. Of course, at lower speeds the damping constant takes on a positive sign. In this range the damper causes a strong increase in the oscillations. At higher speeds, however, the constant is negative, i.e. we get the damping action described above.

The improved safety when the steering damper is used depends, however, less on its property of causing oscillations (which have begun) to die out than on its ability to prevent their occurrence. Experience shows that handlebar shimmy, which first starts with a definite magnitude of deflections, increases so rapidly that the driver can no longer limit it. The hinge then strikes left and right against the stops with great force. The energy transfer is so large that even a fully applied damper might not be able to cause the oscillation to die out fast enough. The threshold to this increase in the oscillations, due to the high rate of energy input, appears to occur when the force transfer, determined by coulomb friction between the front wheel and the road is exceeded (this is hardly to be explained mathematically). In general the steering damper makes it possible to suppress the oscillations excited by the driver or the road as soon as they arise and thus to prevent the danger of steering shimmy.

It still remains to be established, however, that such a steering damper is a really necessary aid inasmuch as it must always be used by the driver when the speed changes as, for example, in passing through populated areas, and its action is also not always sufficient to prevent oscillations. A vehicle ought to be made in such a way that it can do without steering dampers. Under some circumstances the installation of a fluid damper ought to be considered which opposes the rapid shimmy oscillations with high resistance to motion but permits the slow stabilizing motions of the driver at low speeds. Such hydraulic damping which is proportional to the speed could alter the natural frequency of the system even with no other devices.

The theoretical results presented here have been checked and confirmed with measurements⁴⁾.

4) E. Döhning: The Stability of Single-Track Vehicles. Automob. Tech. Z. Vol. 56 (1954) p. 68-72

3. Summary

The known linearized equations of motion for the bicycle have been extended by more precise consideration of the front wheel system. Using them we can investigate the motion of single-track vehicles mathematically. From this, three characteristic types of motion were found. One is damped at higher speeds but has unstable oscillations at lower speeds; a second has a very rapid return to zero for a deflected system; and the third is characterized by a very slow increase at higher speeds and a slow decrease of a deflection at lower speeds. Three speed ranges may be distinguished. In the lowest range, which extends from about 0 to 20 km/hr for common modern vehicles, instability prevails because of the growth of the oscillation. In the middle range, from about 20 to 40 km/hr, the single-track vehicle is theoretically inherently stable. In the upper speed range, at more than about 40 km/hr, a small instability occurs in the form of a very slow increase of any deflection once it starts (amplitude doubles in 5 to 10 seconds). The phases of the steering oscillation and that of the roll motion are shifted with respect to one another.

Measurements confirm that calculation of the motion with the aid of the linearized equations of motion suffices to determine the frequency and damping factor of the oscillation. The influence of the basic parameters on these two factors, which are critical in determining the behavior, can thus be investigated theoretically. This makes it possible to find means for improving the mechanisms of single-track vehicles.